

● *Original Contribution*

## STUDY OF SONOPORATION DYNAMICS AFFECTED BY ULTRASOUND DUTY CYCLE

HUA PAN,\* YUN ZHOU,<sup>†</sup> OLIVIER IZADNEGAHDAR,<sup>†</sup> JIANMIN CUI,\* and CHERI X. DENG<sup>†</sup>

\*Department of Biomedical Engineering, Washington University in St. Louis, St. Louis, MO, USA; and

<sup>†</sup>Department of Biomedical Engineering, Case Western Reserve University, Cleveland, OH, USA

(Received 13 October 2004; revised 14 March 2005; in final form 22 March 2005)

**Abstract**—Sonoporation is the ultrasound-induced membrane porosity and has been investigated as a means for intracellular drug delivery and nonviral gene transfection. The dynamic characteristics of sonoporation, such as formation, duration and resealing of the pores in the cell membrane, determine the process of intracellular uptake of molecules or agents of interest that are otherwise obstructed by the cell membrane barrier. Sonoporation dynamics is also important for postultrasound cell survival. In this study, we investigated the effects of ultrasound duty cycle on sonoporation dynamics using *Xenopus* oocyte as a model system. Transducer with a center frequency of 0.96 MHz was used to generate pulsed ultrasound of desired duty cycle (5%, 10% and 15%) at a pulse repetition frequency of 1 Hz and an acoustic pressure of 0.4 MPa in our experiments. Employing voltage clamp techniques, we measured the transmembrane current as the direct result of decreased membrane resistance due to pore formation induced by ultrasound application. We characterized the sonoporation dynamics from these time-resolved recordings of transmembrane current to indicate cell membrane status, including pore formation, extension and resealing. We observed that the transmembrane current amplitude increased with increasing duty cycle, while the recovering process of membrane pores and cell survival rate decreased at higher duty cycles. (E-mail: cheri.deng@cwru.edu) © 2005 World Federation for Ultrasound in Medicine & Biology.

**Key Words:** Sonoporation, Sonoporation dynamics, Ultrasound, Duty cycle, Cell membrane permeability, Ultrasound contrast agent, Drug delivery, Gene transfection.

### INTRODUCTION

Experimental studies demonstrated that ultrasound application allows intracellular uptake of drugs, macromolecules, DNA and fluorescent markers that are otherwise not permeable through the intact cell membrane (Miller et al. 2002; Greenleaf et al. 1998; Shohet et al. 2000; Christiansen et al. 2003; Bekeredjian et al. 2003; Zarnitsyn et al. 2004). Sonoporation, which describes the formation of pores or openings in the cell membrane due to ultrasound exposure (Tachibana et al. 1999; Ward et al. 2000), permits easier inward transport of molecules or other agents of interest into the cells across the membrane barrier, resulting in faster and more direct intracellular uptake.

Sonoporation offers an advantageous intracellular delivery strategy compared with other techniques, such as electroporation (Rystten et al. 2000; Prausnitz

et al. 1993) or viral gene transfection, since the non-ionizing ultrasound method can be noninvasive, a property promising for *in vivo* application (Shohet et al. 2000; Christiansen et al. 2003; Bekeredjian et al. 2003). However, challenges remain to achieve controllable and consistent delivery outcome despite the progress made recently in the field. The mechanism and process of sonoporation have not been understood completely. The dynamics of sonoporation at the cellular level has not been studied, due to the lack of methods for real-time monitoring of sonoporation. Postultrasound assays cannot provide sufficient information to reveal direct correlation of delivery outcome with sonoporation dynamics; therefore, postultrasound analysis alone is insufficient to provide effective guidance to select optimal parameters and conditions to improve delivery efficiency and minimize unwanted side-effects, such as cell lysis (Miller and Quddus 2001) and apoptosis (Feril et al. 2003; Honda et al. 2004).

Reversible sonoporation, during which pores form and subsequently reseal after ultrasound expo-

Address correspondence to: Cheri X. Deng, Ph.D., Department of Biomedical Engineering, Case Western Reserve University, Cleveland, OH 44106-7207, USA. E-mail: cheri.deng@cwru.edu

sure, is necessary for cells to survive and maintain viability. Reversible sonoporation is therefore of special interest for successful intracellular drug and gene delivery and for applications involving intracellular transport of molecules or compounds in various formulations with desirable therapeutic and diagnostic/imaging capabilities. On the other hand, irreversible sonoporation occurs when the pores do not reseal efficiently and properly. In such cases, the cells cannot recover from the ultrasound-induced membrane disruption and cell death occurs as a result (Keyhani et al. 2001).

The dynamics of sonoporation process including pore formation, extension, duration and resealing, directly defines the entry pathway of extracellular agents or molecules and the likelihood of cell recovery. Sonoporation may also trigger other complex cellular processes that affect cell fate. Therefore, ultrasound-mediated intracellular delivery outcome, denoted by delivery efficiency and postultrasound cell survival, will depend on the dynamic characteristics of the sonoporation.

Both continuous wave (CW, or tone burst) ultrasound and pulsed ultrasound exposures have been used for sonoporation. It is expected that a longer ultrasound application time might increase the chance for higher delivery efficiency. However, long duration of ultrasound exposure increases the likelihood of undesirable and irreversible damage to cells which eventually lead to cell death. It is especially important to avoid the unwanted effects such as mechanical and thermal damage to tissue due to prolonged exposure of high intensity ultrasound for *in vivo* applications (Barnett et al. 1994).

At duty cycles lower than 100%, pulsed ultrasound has a lower temporal-averaged intensity than tone burst exposures at the same peak intensity. For intracellular transport *via* sonoporation, spreading the total ultrasound energy over a longer period of time will be beneficial if enhanced cell permeability can be maintained during that period. Such prolonged cell porosity might be necessary to allow sufficient intracellular transport of desirable payload to be achieved. Furthermore, diagnostic ultrasound, which operates in pulse-echo mode at a low duty cycle, has been used for sonoporation (Shohet et al. 2000; Miller and Quddus 2000; Miller and Quddus 2001; Miller et al. 2003) with additional advantage, with its real-time imaging capability for guided application.

The difference in the dynamics of sonoporation has not been studied in the cellular level to elucidate how the different exposure protocols (CW or pulsed ultrasound) affect delivery outcome. Our recent study (Deng et al. 2004) revealed dynamic characteristics of

sonoporation using single *Xenopus* oocyte as a model system exposed to tone burst ultrasound of 0.5s duration. We demonstrated that increasing acoustic pressure results in increasing transmembrane current and also measured the time constant of 2 to 8 s of resealing. Our results demonstrated successful real-time measurement of sonoporation by employing voltage clamp techniques (Hille 2001); the transmembrane current change directly correlates with the membrane porosity induced by ultrasound, providing a real-time, sensitive monitoring of membrane pore formation and resealing in sonoporation.

In this paper, we report our experimental study of the effects of pulsed ultrasound duty cycle on sonoporation dynamics, which may help to obtain an improved understanding of sonoporation mechanism.

## MATERIALS AND METHODS

We employed voltage clamp techniques (Hille 2001) to monitor in real-time the changes in cell membrane induced by ultrasound application using *Xenopus* oocytes as a model system (Deng et al. 2004; Shi et al. 2002; Masu et al. 1987). The same animal protocol and experimental set-up as described in our previous paper (Deng et al. 2004) were used for this study and is summarized in the following.

### *Xenopus oocytes preparation*

The procedures on harvesting and preparation of *Xenopus* oocytes follow an animal protocol approved by our Institutional Animal Care and Use Committee. Adult female *Xenopus laevis* (NASCO, Fort Atkinson, WI, USA) was anaesthetized by immersing in 0.3% tricaine (Sigma, St. Louis, MO, USA) solution for 20 min. Oocytes were taken from a small incision (0.5 to 1 cm) made in the frog's lower abdomen, which was then sutured back. The toad was allowed to recover in fresh water. Oocytes were digested in collagenase (2 mg/mL in ND96 solution that contains in mM 96 NaCl, 2 KCl, 1.8 CaCl<sub>2</sub>, 1 MgCl<sub>2</sub>, 5 HEPES, pH 7.60) for defolliculation. They were used immediately in experiments or stored in ND96 solution at 18°C for 1 or 2 d before use.

### *Experiment set-up for real-time measurement of sonoporation*

A cylindrical chamber (radius of 1.5 cm and depth of 0.3 cm) with an acoustically transparent bottom (thin plastic film) was used to hold a single *Xenopus* oocyte (diameter ~ 0.7 mm) bathed in ND96 solution. Optison™, a microbubble ultrasound contrast agent with a mean diameter of 3 μm (original concentration ~ 5 × 10<sup>8</sup> particles/mL) (Amersham

Health, Princeton, NJ, USA), was diluted in ND96 solution by mixing the original stock solution drawn from a vial with ND96 solution and was added into the bath to facilitate sonoporation. The mixture was examined before and after ultrasound experiment under microscope and bubble concentration was confirmed by counting.

The ultrasound system includes a function/waveform generator (33250A, Agilent Technologies, Palo Alto, CA, USA), a 75-W power amplifier (75A250, Amplifier Research, Souderton, PA, USA) and a custom-made circular planar piezoelectric ultrasound transducer (diameter 5.1 cm, center frequency 0.96 MHz). The ultrasound output was calibrated using an ultrasound power meter (UPM-DT-10, Ohmic Instrument Co., Easton, MD, USA) and the amplitude of acoustic pressure inside the chamber was measured using a 40- $\mu\text{m}$  calibrated needle hydrophone (HPM04/1, Precision Acoustics, UK).

Microelectrodes (tip diameter  $\sim 1 \mu\text{m}$ ) were pulled from glass pipette (Warner Instrument Corp., Hamden, CT, USA) using an electrode puller (Sutter Instrument Co., Novato, CA, USA). They were filled with 3 mol/L KCl and had resistances between 0.5 to 1.0 mol/L $\Omega$ . Two microelectrodes were inserted into the oocyte membrane and connected to a voltage clamp amplifier (Dagan CA-1B, Dagan Corp., Minneapolis, MN, USA) (Stuhmer 1998) to measure the transmembrane current when the membrane potential of the oocyte was clamped at  $-50 \text{ mV}$  during recordings. Trigger signals from the voltage clamp system are used to control ultrasound activation to allow correlated real-time recording of transmembrane current of a single oocyte before, during and after ultrasound application.

No change in the transmembrane current was observed without ultrasound application or with ultrasound application in the absence of Optison<sup>TM</sup>. On the other hand, we have consistently observed that ultrasound application (0.4 MPa) induces increased inward transmembrane current in the presence of Optison<sup>TM</sup> (Deng *et al.* 2004).

## RESULTS

Monitoring of sonoporation using two-electrode voltage clamp readily measures the membrane status in real time. Figure 1 shows the transmembrane current measured in an oocyte exposed to pulsed ultrasound at a duty cycle 10% and a pulse repetition frequency (PRF) of 1 Hz. The Optison concentration was 10% and the acoustic pressure was 0.4 MPa. Marked difference in the dynamics of sonoporation in the cellular level between tone-burst ultrasound (Deng

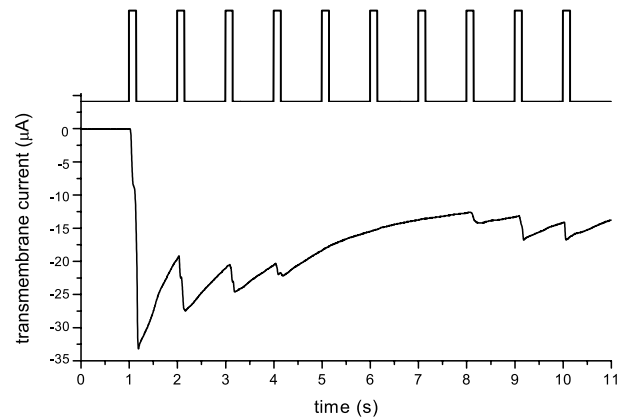


Fig. 1. Transmembrane current measured in an oocyte exposed to pulsed ultrasound exposure at a duty cycle 10% and a pulse repetition frequency (PRF) of 1 Hz. Acoustic pressure amplitude of ultrasound was 0.4 MPa. Optison<sup>TM</sup> concentration was 10%.

*et al.* 2004) and pulsed ultrasound is clearly demonstrated when the transmembrane currents are compared. During the tone burst application, the transmembrane current increased continuously until ultrasound was terminated and then underwent a monotonic declination (recovery to the equilibrium level), indicating the resealing of the membrane. During the pulsed ultrasound exposure, the amplitude of the current increased at the beginning of most discrete pulses and started to recover during the silent interval until the next pulse, allowing the membrane to reseal partially.

To quantitatively characterize the sonoporation dynamics affected by pulsed ultrasound systematically, we exposed *Xenopus* oocytes to pulsed ultrasound of duty cycles of 5%, 10% and 15%. With a constant pulse repetition frequency (PRF) of 1 Hz, the corresponding pulse length was 0.05s, 0.1s and 0.15 s, respectively. The total duration of ultrasound activation was kept at 10 s and the acoustic pressure at 0.4 MPa. Optison<sup>TM</sup> concentration (5%) was kept constant for these experiments.

From the measured transmembrane currents which resulted from pulsed ultrasound exposures of different duty cycles (Fig. 2), several parameters are computed quantitatively to assay the cell's dynamic states during sonoporation. The maximum current change (Fig. 3) denotes the maximum amplitude of the ionic current through the membrane. Since the pulse repetition period ( $\text{PRT} = 1/\text{PRF}$ ) was fixed at 1 s, an increase in duty cycle creates longer duration for each discrete pulse, which generates larger transmembrane increase, as reported previously (Deng *et al.* 2004).

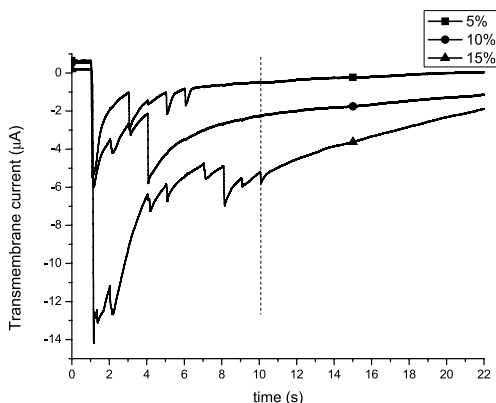


Fig. 2. Transmembrane current as the result of pulsed ultrasound exposures at different duty cycles (5% to 15% as shown) in the presence of Optison (5%). Ultrasound center frequency was 0.96 MHz and the PRF 1 Hz. Ultrasound application time was 10 s and acoustic pressure was 0.4 MPa. The dashed vertical line at 10 s indicates the end of ultrasound application.

Figure 3 shows an expected increase of maximum current change with increasing duty cycle.

The total ionic transfer, which measures the total amount of electric charges crossing the membrane during a period of time (20 s), is evaluated by integrating the measured transmembrane current over the time period as  $Q = \int_{t_1}^{t_2} I(t)dt$ , where  $I(t)$  is the time-dependent transmembrane current in  $\mu A$ . The total ionic transfer at different duty cycles is shown in Fig. 4 and exhibits an increase of ionic inflow with increasing duty cycle, confirmed by a Student's  $t$ -test ( $n = 7, 9, 11$ ) with 95% confidence level. These results (Figs. 3 and 4) indicate that a higher duty cycle resulted

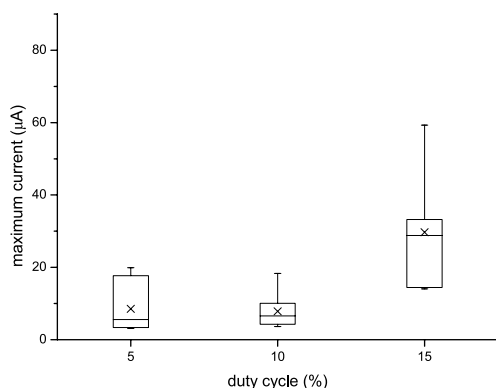


Fig. 3. The maximum current change at three duty cycles. Numbers of measurements are  $n = 7$  (5%), 7 (10%), 8 (15%). The PRF = 1Hz, the ultrasound application time was 10 s and acoustic pressure was 0.4 MPa. Optison™ concentration was 5%. In this and other figures, the lines in box plots correspond to maximum value, minimum value, 75 percentile, median and 25 percentile in the results. The x represents the mean of data.

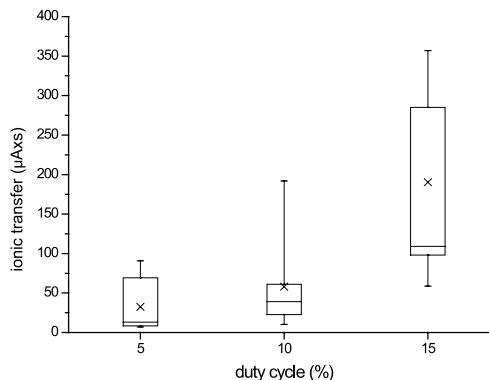


Fig. 4. The total ionic transfer (integration of transmembrane current over time) vs. duty cycle. The ultrasound parameters are the same as in Figure 5. Numbers of measurements are  $n = 7$  (5%), 7 (10%) and 8 (15%).

higher level of cell membrane porosity (larger total area of pores, *i.e.*, more pores or pores with a larger size) in the membrane, as well as longer lasting openings.

The cumulative ion transfer, defined and calculated as the integration of the transmembrane current over time  $A(t) = \int_{t_0}^t I(t)dt$ , denotes the ionic translocation into the cell at each time point (Fig. 5). The result shows that the cumulative ionic transfer increases with time, even after the ultrasound protocol was terminated ( $t = 11.5$  s) because it took time for the membrane to reseal eventually. Therefore, due to the time course of resealing, the membrane will remain permeable for a period of time for substance delivery after the ultrasound protocol is terminated. It is also noted that the increment of cumulative ion transfer had a higher rate at higher duty cycles.

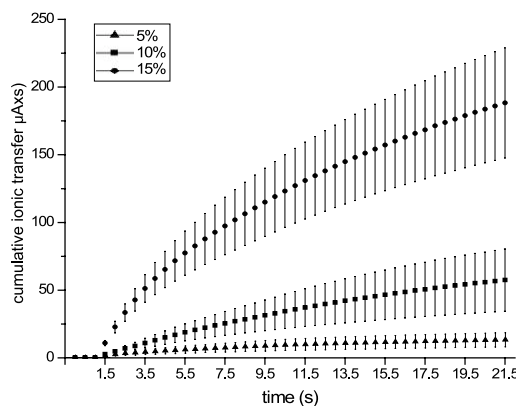


Fig. 5. The cumulative ion transfer vs. time at different duty cycles. The cumulative ion transfer is calculated as the area under the curve of the transmembrane current at a given time. The other parameters are the same as in Figure 5.

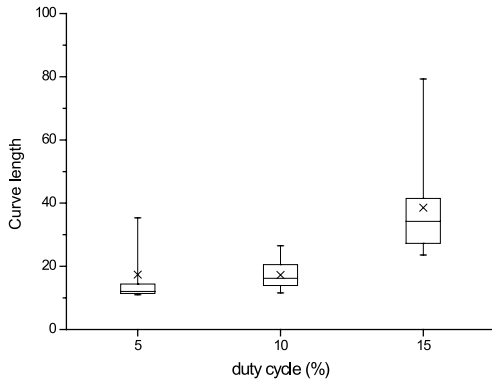


Fig. 6. The current-time curve length (CTCL) within 20 s after ultrasound activation vs. duty cycle. The other parameters are the same as in Figure 5.

The current-time curve length (CTCL) measures the length of the curve representing the dynamics of transmembrane current change over a period of time (*e.g.*, 20 s) after ultrasound activation. The signal is normalized by the maximum current change to eliminate any ionic or other environment dependence, to obtain more relevant information associated with cell membrane dynamics. The CTCL is computed via the following algorithm  $\int_{t_1}^{t_2} \sqrt{\left(\frac{I(t)}{(\Delta I)_{\max}}\right)^2 + \left(\frac{t}{PRT}\right)^2} dt$ , where  $I(t)$  is the transmembrane current at a particular time  $t$ , the time elapsed after ultrasound activation. Our result shows that the curve length increases with increasing duty cycle (Fig. 6), as more fluctuations are often observed with increasing duty cycle (Fig. 2). Obviously, a constant current change should yield a small curve length. This parameter is recognized to indicate the dynamic plasma membrane disruption and might be related to more complex cellular processes as the cell membrane experiences repeated disruption. As the duty cycle elevates, the cell is being obstructed more from recuperating and, thus, the recovery process is expected to experience more dynamics. While CTCL is not expected to affect delivery efficiency to a significant degree, whether it has implications on ultimate cell fate (survival) requires further study.

We investigated postultrasound cell recovery affected by duty cycles. Figure 7a–7c show the percentage of transmembrane current recovery (from the maximum amplitude) of each oocyte ( $n = 7$ ) at 11 s (the end of ultrasound application), 22 s and 2 min. Higher recovery percentage is observed at lower duty cycle initially (Fig. 7a) and the difference decreases as the cells have more time to recovery (Fig. 7c), indicating that the oocytes recover faster after being exposed to ultrasound at lower duty cycles.

As the membrane must reseal completely for cells to survival, immediate loss of cell viability or short-term cell death can also be assessed from the transmembrane current. Figure 8a shows an example of cell death/nonrecovery of membrane disruption of an oocyte exposure to 15% duty cycle at 0.5 MPa. The current had a considerably slower recovery rate and did not recover completely to the starting level after an extended period of time (*e.g.*, 5 min or longer) when

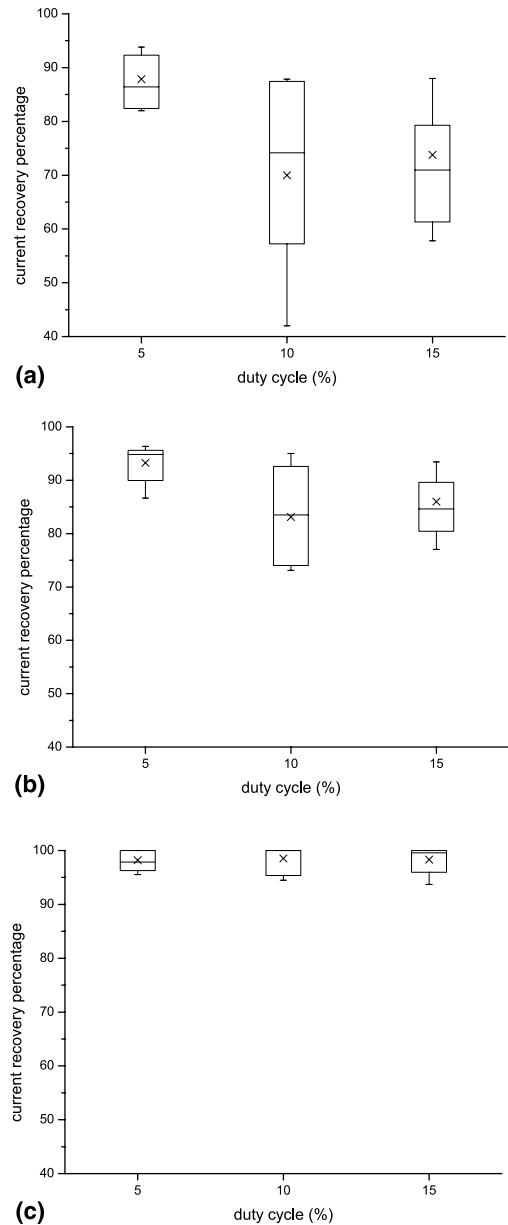


Fig. 7. (a) Percentage of transmembrane current recovery vs. duty cycle at the end of ultrasound application (10 s). (b) Percentage of transmembrane current recovery after 20 s after ultrasound application. (c) Percentage of transmembrane current recovery after 2 min of ultrasound application.



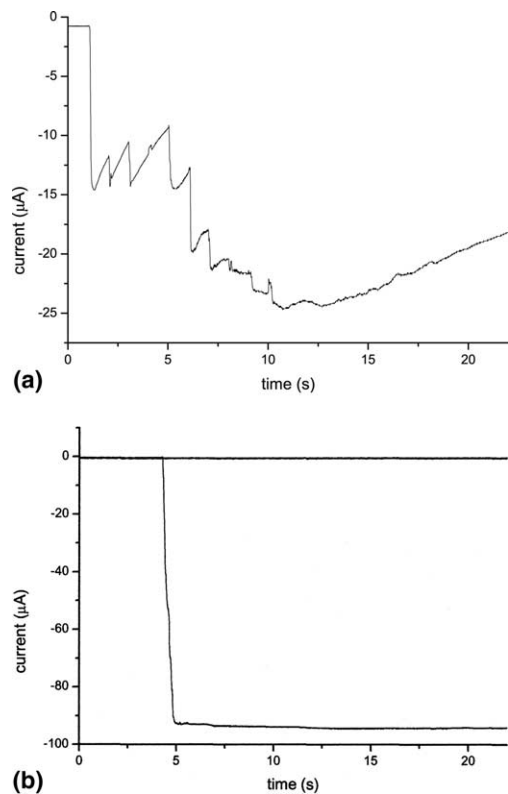


Fig. 8. (a) An example of cell death/nonrecovery of membrane disruption of an oocyte exposed to ultrasound at 0.4 MPa and at 15% duty cycle. (b) Cell death for a tone burst ultrasound exposure at the same acoustic pressure amplitude lasting 1 s.

the cell was confirmed dead. For a tone burst exposure at the same acoustic pressure amplitude lasting 1 s, the inward transmembrane current had a much more rapid and larger increase and no recovery was observed, shown in Fig. 8b. Cell death was immediately confirmed from microscope examination. We examined cell death rate for different duty cycles (at 0.4 MPa) and noted a decrease in cell survival rate at higher duty cycle, shown in Table 1.

## SUMMARY AND DISCUSSION

The sonoporation dynamics affect the delivery efficiency, because the dynamic behaviour of pores directly defines the time window for entry of extracellular agents or molecules into the cells. The characteristics of pores also determine the cell viability, because cell survival relies on the resealing of membrane disruption.

Our previous study has characterized the dynamic process of sonoporation of oocyte membrane exposed to a tone burst ultrasound (Deng et al. 2004) and found that the membrane resealing initiates at the end of tone burst ultrasound application and has a recovery time

constant in the order of 2 to 8 s. To extend the time duration of cell membrane porosity to improve delivery outcome, pulsed ultrasound can be exploited for sonoporation. In this study, we studied the sonoporation dynamic process affected by pulsed ultrasound duty cycle, while keeping other parameters, such as the acoustic pressure amplitude, constant. Our results demonstrate marked differences in the dynamics of pulsed ultrasound induced-membrane status (Figs. 3 and 4) compared with tone-burst ultrasound exposures (Deng et al. 2004), notably a longer duration of enhanced cell porosity even for the same total effective ultrasound exposure time (e.g., 1 s for a 10 s ultrasound application at 10% duty cycle). The spreading of energy over a longer duration helps to avoid the extension of pores to sizes too large and/or the formation of too many more pores that might more easily lead to irreversible sonoporation. We have consistently observed that a 1 s tone-burst exposure under the same conditions (0.4 MPa and 5% Optison™ concentration) always cause irreversible membrane disruption and immediate cell death (Fig. 8b). Meanwhile, since the pores will not reseal completely during the interval of pulses, the membrane can remain porous during the entire ultrasound application duration, creating a prolonged time window of enhanced cell porosity. We have noticed that the transmembrane current does not always exhibit increase at the beginning of each pulse. This is attributed to the unavailability of microbubbles in the cell vicinity; this is especially true near the later stage of ultrasound application, where less microbubbles are available, due to destruction already occurred.

We characterized quantitatively the sonoporation dynamics affected by duty cycle in several different aspects, illustrated by the parameters shown in Figs. 3 to 7. The parameters directly reflect the total area of the pores formed in the membrane and the duration of the pores remaining open, which will determine delivery efficiency. In the voltage clamp experiments, the increasing maximum current and the total ionic transfer (related to the measured current) are used as indicators to demonstrate the cell porosity and, therefore, the dependence of the delivery efficiency with increasing duty cycle (fixed PRF of 1 Hz). A larger total effective ionic transfer at higher duty cycle indicates that the porosity resulting from a higher duty cycle will allow more substance to be delivered during drug

Table 1. Cell survival rate at different duty cycles

Duty cycle	5% ( $n = 7$ )	10% ( $n = 9$ )	15% ( $n = 11$ )
Cell survival rate	100%	78%	73%

or gene delivery. The substance in drug or gene delivery may enter the cell through pores by diffusion due to a higher extracellular concentration.

The cumulative ion transfer describes a time-dependent ionic transfer into the cell and provides a dynamic assessment of intracellular delivery efficiency and is therefore used to gauge the dynamics of the sonoporation process affected by ultrasound duty cycle. The result of increasing cumulative ionic inflow (Fig. 5) with increasing duty cycle is expected and consistent with other parameters related to how duty cycle affects delivery efficiency.

It is also observed in our experiments (Figs. 3 to 7) that there exists considerable variation in the transmembrane current measurements and, thus, variation of the parameters derived. We recognized that this is mainly due to the variation inherent in the condition and properties of individual oocytes and the randomness of microbubble activities near the membrane, related to conditions of microbubbles (*e.g.*, Optison™ dilution). Microbubble contrast agents are used to facilitate the inception of cavitation which is associated with the formation of pores in cell membrane (Miller *et al.* 2002). Uncertainty arises from variation of handling and prolonged open-air environment that might alter the property of the shelled microbubbles during experiment process. Noticeably, bubbles, especially those of larger sizes, tend to float up to the surface of the solution, making the effective bubble concentration and size distribution in the vicinity of the oocyte difficult to predict and control. In our study, effort was made to minimize such alteration by using fresh samples of Optison™ dilution and examining the bubbles under microscope periodically. We also tried evenly to distribute Optison™ bubbles in the bath solution when necessary.

Short-term cell recovery or immediate loss of cell viability after ultrasound can be readily assessed from the transmembrane current dynamics. The nearly 100% current recovery 2 min after ultrasound application (Fig. 7c) correlates well with cell survival, while a prolonged duration or nonrecovery of the current at an elevated level (Fig. 8) indicates acute cell death, when the cell is unable to reseal and repair its membrane disruption. Such correlation of sonoporation dynamics with cell fate may provide insight regarding cell death, such as cell lysis and apoptosis, observed in mammalian cells (Miller and Quddus 2001; Feril *et al.* 2003; Honda *et al.* 2004) which were obtained from postultrasound analysis.

In summary, we have quantitatively characterized sonoporation dynamics in *Xenopus* oocytes exposed to pulsed ultrasound (center frequency 0.98 MHz) at different duty cycles (5%, 10% and 15%) in the pres-

ence of Optison™. From inward transmembrane current measured with the two electrode voltage clamp technique, our results demonstrated that higher duty cycle induces higher level of sonoporation dynamics, demonstrated by the quantitative parameters related to dynamic membrane status. These parameters are indicative parameters that are related to ultrasound delivery efficiency and cell survival.

Future studies include investigation of effects of other parameters on sonoporation dynamics. Studies are needed to demonstrate the direct correlation of sonoporation dynamics with delivery efficiency and longer term cell survival. Studies are underway to investigate sonoporation in mammalian cells by employing the patch clamp technique that is suitable for much smaller-sized mammalian cells.

*Acknowledgements*—This work was supported by grants from the NIH (HL70393) and the Whitaker Foundation (RG 00 to 0396) (to JC) and star-tup funding (to CXD) from the Department of Biomedical Engineering, Case Western Reserve University.

## REFERENCES

- Barnett SB, ter Haar GR, Ziskin MC, Nyborg WL, Maeda K, Bang J. Current status of research on biophysical effects of ultrasound. *Ultrasound Med Biol* 1994;20:205–218.
- Bekeredjian R, Chen S, Frenkel PA, Grayburn PA, Shohet RV. Ultrasound-targeted microbubble destruction can repeatedly direct highly specific plasmid expression to the heart. *Circulation* 2003; 108(8):1022–1026.
- Christiansen JP, Kondo T, French BA, Klivanov AL, Kaul S, Linder JR. Targeted tissue transfection with ultrasound destruction of plasmid-bearing cationic microbubbles. *Ultrasound Med Biol* 2003; 29:1759–1767.
- Deng CX, Seiling F, Pan H, Cui J. Ultrasound induced cell-membrane porosity. *Ultrasound Med Biol* 2004;30:519–526.
- Feril LB, Jr., Kondo T, Zhao QL, *et al.* Enhancement of ultrasound-induced apoptosis and cell lysis by echo-contrast agents. *Ultrasound Med Biol* 2003;29:331–337.
- Greenleaf WJ, Bolander ME, Sarkar G, Goldring MB, Greenleaf JF. Artificial cavitation nuclei significantly enhance acoustically induced cell transfection. *Ultrasound Med Biol* 1998;24:587–595.
- Hille B. *Ion Channels of Excitable Membranes*, 3rd edition. Sunderland MA: Sinauer Associates, Inc., 2001.
- Honda H, Kondo T, Zhao QL, Feril LB, Jr., Kitagawa H. Role of intracellular calcium ions and reactive oxygen species in apoptosis induced by ultrasound. *Ultrasound Med Biol* 2004;30: 683–692.
- Keyhani K, Gusman H, Parsons A, Lewis TN, Prausnitz MR. Intracellular drug delivery using low-frequency ultrasound: quantification of molecular uptake and cell viability. *Pharm Res* 2001;18:1514–1520.
- Masu Y, Nakayama K, Tamaki H, *et al.* cDNA cloning of bovine substance-K receptor through oocyte expression system. *Nature* 1987;329:836–838.
- Miller DL, Quddus J. Sonoporation of monolayer cells by diagnostic ultrasound activation of contrast-agent gas bodies. *Ultrasound Med. Biol* 2000;26:661–667.
- Miller DL, Quddus J. Lysis and sonoporation of epidermoid and phagocytic monolayer cells by diagnostic ultrasound activation of contrast agent gas bodies. *Ultrasound Med Biol* 2001;27:1107–1113.

- Miller DL, Pislaru SV, Greenleaf JE. Sonoporation: Mechanical DNA delivery by ultrasonic cavitation. *Somat Cell Mol Genet* 2002;27:115–134.
- Miller DL, Dou C, Song J. DNA transfer and cell killing in epidermoid cells by diagnostic ultrasound activation of contrast agent gas bodies in vitro. *Ultrasound Med Biol* 2003;29:601–607.
- Prausnitz MR, Lau BS, Milano CD, Conner S, Langer R, Weaver JC. A quantitative study of electroporation showing a plateau in net molecular transport. *Biophys. J.* 1993;65:414–422.
- Ryttsen F, Farre C, Brennan C, et al. Characterization of single-cell electroporation by using patch-clamp and fluorescence microscopy. *Biophys J* 2000;79:1993–2001.
- Shi J, Krishnamoorthy G, Yang Y, et al. Mechanism of magnesium activation of calcium-activated potassium channels. *Nature* 2002;418:876–880.
- Shohet RV, Chen S, Zhou YT, et al. Echocardiographic destruction of albumin microbubbles directs gene delivery to the myocardium. *Circulation* 2000;101:2554–2556.
- Stuhmer W. Electrophysiologic recordings from *Xenopus* oocytes. *Methods Enzymol* 1998;293:280–300.
- Tachibana K, Uchida T, Ogawa K, Yamashita N, Tamura K. Induction of cell-membrane porosity by ultrasound. *Lancet* 1999;353:1409.
- Ward M, Wu J, Chiu JF. Experimental study of the effects of Optison® concentration on sonoporation in vitro. *Ultrasound Med Biol* 2000;26:1169–1175.
- Zarnitsyn VG, Prausnitz M. Physical parameters influencing optimization of ultrasound-mediated DNA transfection. *Ultrasound Med Biol* 2004;30:527–538.